Published in final edited form as:
Cancer Res. 2013 September 1; 73(17): 5371–5380. doi:10.1158/0008-5472.CAN-12-4707.

Candidate tumor suppressor and pVHL partner Jade-1 binds and inhibits AKT in renal cell carcinoma

Liling Zeng[1], **Ming Bai**[2], **Amit K. Mittal**[1], **Wassim El-Jouni**[3], **Jing Zhou**[3], **David M. Cohen**[4], **Mina I. Zhou**[1], and **Herbert T. Cohen**[1]

[1] Renal and Hematology/Oncology Sections, Departments of Medicine and Pathology, Boston Medical Center and Boston University School of Medicine, Boston, MA 02118 USA

[2] Division of Rheumatology, Immunology and Allergy, Department of Medicine, Brigham and Women's Hospital and Harvard Medical School, Boston, MA 02115 USA

[3] Renal Division, Department of Medicine, Brigham and Women's Hospital and Harvard Medical School, Boston, MA 02115 USA

[4] Division of Nephrology & Hypertension, Department of Medicine, Oregon Health Science University, Portland, OR 97239 USA

Abstract

The von Hippel-Lindau tumor suppressor pVHL (VHL) is lost in the majority of clear-cell renal cell carcinomas (RCCs). Activation of the PI3K/AKT/mTOR pathway is also common in RCC, with PTEN loss occurring in ~30% of the cases, but other mechanisms responsible for activating AKT at a wider level in this setting are undefined. Plant homeodomain protein Jade-1 (PHF17) is a candidate renal tumor suppressor stabilized by pVHL. Here using kinase arrays we identified phospho-AKT1 as an important target of Jade-1. Overexpressing or silencing Jade-1 in RCC cells increased or decreased levels of endogenous phospho-AKT/AKT1. Further, reintroducing pVHL into RCC cells increased endogenous Jade-1 and suppressed endogenous levels of phospho-AKT, which colocalized with and bound to Jade-1. The N-terminus of Jade-1 bound both the catalytic domain and the C-terminal regulatory tail of AKT, suggesting a mechanism through which Jade-1 inhibited AKT kinase activity. Intriguingly, RCC precursor cells where Jade-1 was silenced exhibited an increased capacity for AKT-dependent anchorage-independent growth, in support of a tumor suppressor function for Jade-1 in RCC. In support of this concept, an in silico expression analysis suggested that reduced Jade-1 expression is a poor prognostic factor in clear-cell RCC that is associated with activation of an AKT1 target gene signature. Taken together, our results identify two mechanisms for Jade-1 fine control of AKT/AKT1 in RCC, through loss of pVHL, which decreases Jade-1 protein, or through attenuation in Jade-1 expression. These findings help explain the pathologic cooperativity in clear-cell RCC between PTEN inactivation and pVHL loss, which leads to decreased Jade-1 levels that superactivate AKT. Additionally, they prompt further investigation of Jade-1 as a candidate biomarker and tumor suppressor in clear-cell RCC.

Keywords

Jade-1; AKT; pVHL; renal tumor suppressor; anchorage-independent growth

Corresponding author: Herbert T. Cohen, 650 Albany Street, Rm X-535, Boston, MA 02118; Phone: 617-638-7322, Fax: 617-638-7326, htcohen@bu.edu.

Conflicts of Interest: The authors disclose no potential conflicts of interest.

Introduction

Renal cancer is a major clinical problem (1). In the US, 65,150 new cases and 13,680 deaths were predicted from cancer of the kidney and renal pelvis for 2013 (2). More than 90% of kidney cancers are believed to originate from renal epithelial cells and are therefore referred to as renal-cell carcinomas (RCCs) (3). The majority of cases of clear-cell RCC, the most common subtype of RCC, are characterized genetically by the loss, mutation or silencing of the *VHL* gene (4, 5), making pVHL the major renal tumor suppressor in adults. However, the pathogenesis of renal cancer remains unresolved.

Serine/threonine kinase AKT is a key factor of perhaps the most frequently activated proliferation and survival pathway in cancer (6). Elevated AKT activity is also found in RCC and kidney cysts. Cystic lesions of VHL patients show hyperactivated PI3K/AKT signaling (7). Increased phospho-AKT levels were found in about 50% of RCC tumor samples, and most commonly in the clear-cell subtype (8). Combined mutations of *VHL* and *PTEN*, a phosphatidylinositol (3,4,5)-trisphosphate phosphatase which negatively regulates AKT/PKB signaling pathway, leads to kidney cysts in mice (7). PTEN inactivating mutations (9, 10) or decreased PTEN expression have been identified in about 30% of clear-cell RCCs (11-13). Hyperactivation of AKT due to conditional knockout of *neurofibromatosis type 2* in mouse renal proximal tubules leads to invasive RCC (14). Human renal cancer cell lines also show constitutive activation of AKT, and PI3K/AKT inhibitor treatment induces apoptosis and inhibits cell growth *in vitro* and in xenografts (15). Thus, AKT is activated in clear-cell RCC, but the mechanism has not always been apparent.

Jade-1, a short-lived protein most highly expressed in renal proximal tubules, was identified as a novel strong binding partner of pVHL (16). Wild-type pVHL stabilizes Jade-1, while renal cancer-causing forms cannot (17). Jade-1 is a candidate renal tumor suppressor and promotes apoptosis (18). Jade-1 functions as a ubiquitin ligase to inhibit canonical Wnt signaling (19) and as a transcription factor associated with histone acetyltransferase activity (20) and with increased abundance of cyclin-dependent kinase inhibitor p21 (21). Low Jade-1 and high beta-catenin levels by immunohistochemistry have been linked to poor prognosis in renal cancer (22). Jade-1 is highly conserved through vertebrate species (23) and to a lesser degree down to yeast. The *Drosophila Jade-1* ortholog, *Rhinoceros* (*rno*), can antagonize Ras signaling in eye development (24). The *Y53G8AR.2* gene, the *Jade-1* ortholog in *C. elegans*, antagonizes synthetic multivulva gene activities (25). These observations suggest Jade-1 may have additional roles in cellular signal transduction.

To identify novel downstream effectors of pVHL and Jade-1, we used kinase arrays to screen for signaling pathways in which Jade-1 may be involved during renal cancer pathogenesis and identify the AKT/AKT1 pathway as a pVHL and Jade-1 target.

Materials and Methods

Constructs

For pSUPER*Jade-1*sh (for constant *Jade-1* knockdown) or pSUPERIOR.neo*Jade-1*sh (for inducible *Jade-1* knockdown) constructs, siRNA duplex DNA oligomers (sequences can be obtained from the authors) were ligated into pSUPER or pSUPERIOR.neo vector (OligoEngine, Seattle, WA) using BglII and HindIII sites. p*Jade-1*sh1, p*Jade-1*sh2 and non-silencing vector were from Open Biosystems/Thermo Scientific. Flag-Jade-1 plasmid, myc-Jade-1 full length and deletion mutants del1, del2, del3, del4, J-N, J-La, and J-Sm have been described in (16, 19, 21). Adenovirus expressing myrAKT, dnAKT or control β-gal was described in (26). pCMV5-based HA-AKT constructs were generated by site-directed mutations: dd (T308D/S473D), aa (T308A/S473A), and ki (K179M). To make GST-tagged

AKT-P/L, AKT-cat, and AKT-tail constructs, AKT nucleotide sequences encoding aas 1-143, 144-349, or 350-480 (27) were PCR-cloned into vector pGEX-6P-1 using BamHI and SalI sites.

Antibodies

Anti-Jade-1 rabbit polyclonal serum was described in (16). AKT, phospho-AKT S473, phospho-AKT T308, AKT1, AKT2, phospho-AKT substrate (RXRXXS*/T*), GSK3β, phospho-GSK3β Ser9, Erk1/2, pErk1/2, HA and myc antibodies were from Cell Signaling. pVHL and p21 antibodies were from BD Pharmingen.

Cell culture and establishment of stable cell lines

HEK293, HEK293T17 and HK-2 cell lines were purchased from American Type Culture Collection and cultured as described (19). 786-O stable cell lines were described in (16). To make tet-inducible *Jade-1* knockdown cell lines, pSUPERIOR.neo*Jade-1*sh was stably transfected into tet-responsive HEK293 cells stably overexpressing the Tet repressor (Invitrogen). Cells were maintained with 2 μg/mL blasticidin and 200 μg/mL G418. HEK293 Flag-Jade-1 stable cells were maintained with 100 μg/mL hygromycin B. HK-2 cells were transduced with p*Jade-1*sh1, p*Jade-1*sh2 or non-silencing-containing viral particles produced from a lentivirus-based packaging system and were maintained with 2 μg/mL puromycin.

MAPK array assay and AKT kinase assay

The Proteome Profiler Human phospho-MAPK Array Kit was from R&D Systems. The AKT kinase assay kit was from Cell Signaling. Kits were used as indicated by the manufacturers.

Cell-growth assay and anchorage-independent growth assay

The cell-growth assay was described in (18). For the anchorage-independent growth assay, 24,000 cells per 35 mm well were diluted in 0.4% agarose in complete medium on top of a 1% agarose layer. Cells were incubated at 37°C 5% CO_2, and fresh medium was added every four days. Foci were then counted under microscopy.

Gene expression analysis of clear-cell RCCs

The Cancer Genome Atlas database (https://tcga-data.nci.nih.gov/tcga/) of 464 clear-cell RCCs generated using the Illumina HiSeq platform was employed to investigate the association of transcript levels of *Jade-1* and *AKT1* with patient clinical characteristics. Significance Analysis of Microarrays of Biometric Research Branch (BRB) Array tools (http://linus.nci.nih.gov/BRB-ArrayTools.html) and students' T-test ($p<0.05$) were used to identify significantly differentially expressed genes. Chi square and Kaplan-Meier log rank tests were used to compare patient characteristics and survival analysis with Statistical Package for the Social Sciences (SPSS) statistics v20 program.

Results

Jade-1 inhibits phospho-AKT/AKT1 in renal cell lines

Because Jade-1 orthologs participate in signal transduction, we used a phospho-MAPK array kit to look for signaling pathways in which Jade-1 is involved. In tet-inducible *Jade-1* knockdown HEK293 cells, tetracycline treatment induced *Jade-1* shRNA expression, such that the endogenous level of Jade-1 was knocked down to 40% compared to a control without tet (Figure 1A, left panel). With *Jade-1* knockdown, the level of endogenous phospho-AKT1 increased by 2.3 fold (Figure 1B, upper panels). Conversely, stable

overexpression of Jade-1 (Figure 1A, right panel) decreased the level of endogenous phospho-AKT1 to 40% compared with empty vector control (Figure 1B, lower panels). phospho-AKT2 was also regulated similarly by Jade-1 but to a lesser degree (Figure 1B), while phospho-p38α9 (T180/Y182) and phospho-p38γ (T183/Y185) were not regulated by Jade-1 (data not shown).

Observations with the phospho-MAPK array were confirmed in transient transfection experiments. Knockdown of *Jade-1* with pSUPER*Jade-1*sh enhanced endogenous AKT1 S473 and T308 phosphorylation by two fold (Figure 1C). Endogenous phospho-AKT2 was only slightly increased with *Jade-1* knockdown, and endogenous pErk1/2 (Erk1 T202/Y204, Erk2 T185/Y187) was not affected by *Jade-1* knockdown. Overexpression of Jade-1 decreased the endogenous phospho-AKT1 level to 30% of control (Figure 1D, left panels). Reintroduction of Jade-1 into the *Jade-1* knockdown cells restored the endogenous phospho-AKT1 levels (Figure 1D, right panels). Thus, Jade-1 specifically regulates phospho-AKT1 without affecting the total endogenous AKT1 level.

To increase efficiency of *Jade-1* knockdown in a model more relevant to renal cancer, we used lentivirus-mediated knockdown in HK-2 cells, a differentiated human proximal tubule cell line (28) that represents a model of renal cancer precursor cells. In *Jade-1*-silenced *Jade-1*sh1 and *Jade-1*sh2 HK-2 cell lines, levels of endogenous phospho-AKT1 S473 and T308 increased about two fold, and total AKT1 levels remained unchanged (Figure 1E). Strikingly, *Jade-1* silencing increased total endogenous phospho-AKT levels by 2-3 fold (Figure 2A). Regulation of phospho-AKT by Jade-1 was inhibited by PI3K inhibitors wortmannin and LY294002. In contrast, endogenous pErk1/2 was not affected by *Jade-1* silencing in the absence or presence of LY294002. In addition, reintroduction of silencing-resistant pFlag-Jade-1 into the *Jade-1*-sh2 cells decreased the levels of phospho-AKT to 50% (Figure 2B).

We also examined phospho-AKT during IGF-1 treatment. phospho-AKT in non-silencing cells was fully activated within 5 minutes. In comparison, phospho-AKT levels in *Jade-1*-sh1 cells increased gradually and reached a two-fold maximum level (compared to non-silencing cells) in 30 minutes (Figure 2C).

We examined the effects of Jade-1 and pVHL on phospho-AKT in 786-O renal cancer cells. Stable overexpression of Jade-1 in 786-O renal cancer cells inhibited endogenous phospho-AKT (Figure 2D). Pooled 786-O stable cell lines expressing either empty vector or HA-tagged pVHL were also established. As expected, stable introduction of pVHL into 786-O cells increased endogenous Jade-1 and decreased endogenous phospho-AKT (Figure 2E). Moreover, the 786-O control cells showed increasing phospho-AKT levels as confluence progressed, whereas the 786-O VHL cells maintained low phospho-AKT levels (Figure 2E). Silencing of *Jade-1* in the 786-O VHL cells increased phospho-AKT levels (Figure 2F), suggesting the effect of pVHL on AKT is Jade-1 dependent. Thus, the regulation of phospho-AKT by Jade-1 is valid, specific and relevant to renal cancer.

Jade-1 interacts with AKT

Endogenous Jade-1 was co-immunoprecipitated with endogenous AKT and *vice versa* (Figure 3A). Confocal microscopy revealed that Jade-1 partly colocalized with AKT. This colocalization was observed inside the cell, in the cytoplasm and nucleus, when cells were at low confluence (Figure 3B), or more consistently near the cell membrane when cells were at confluence (Figure 3C).

To map the AKT-binding domain of Jade-1, HA-AKT1 was co-expressed with deletion/truncation mutants of myc-Jade-1 (Figure 4A). AKT1 only binds full-length, del3 and del4,

but not del1 or del2 (Figure 4B, left panel). AKT1 only binds the Jade-1 N terminus (although with a reduced affinity compared to full-length Jade-1), but not the double-PHD domain J-La or the interfinger region J-Sm (Figure 4B, right panel). Collectively, the N terminus of Jade-1 appears to be necessary for binding AKT1. Kinase inactive (ki) AKT shows much stronger binding with Jade-1 than other forms of AKT (wt, dd, aa) (Figure 4C), implying that Jade-1 makes important and potentially functional contact with the AKT catalytic domain. To determine the Jade-1-binding domain of AKT, myc-Jade-1 was incubated with GST, GST-AKT-PH/Linker, GST-cat, or GST-tail (Figure 4A). Only the AKT catalytic domain and C-terminal tail can bind myc-Jade-1 (Figure 4D). Thus, Jade-1 likely inhibits AKT kinase activity by binding both the AKT kinase domain and regulatory tail.

We also tested whether AKT could be a ubiquitylation target of Jade-1, which is an E3 ubiquitin ligase for the oncoprotein β-catenin (19). Ubiquitylated AKT was not detectable when HEK293 cells were transfected with Jade-1 and/or treated with proteasome inhibitor MG132 (data not shown). Our data also showed that Jade-1 did not affect the total AKT level. Thus, Jade-1 regulates AKT by binding AKT and inhibiting phospho-AKT, but not through AKT ubiquitylation.

Jade-1 silencing affects AKT kinase activity and downstream targets

Next, we examined the molecular effects of elevated levels of phospho-AKT in *Jade-1*-silenced HK-2 cells. AKT *in vitro* kinase assays confirmed elevated AKT kinase activity in *Jade-1*-silenced cells on purified GSK3β (Figure 5A). phospho-AKT substrate (RXRXXS*/T*) antibody was then used to profile phospho-AKT substrates in the HK-2 cell lines. *Jade-1* silencing enhanced several endogenous phospho-substrates of AKT without changing global AKT substrate phosphorylation (Figure 5B), demonstrating selective modulation of AKT substrates in these renal cancer precursor cell lines. As one example, *Jade-1* silencing increased levels of endogenous phospho-GSK3β S9 (Figure 5C). Levels of endogenous p21, a downstream target (29) negatively regulated by phospho-AKT (30, 31), decreased to 40-50% in *Jade-1*-silenced cells (Figure 5D). This effect was attenuated with LY294002. Thus, Jade-1 affects AKT activity and downstream targets.

Jade-1 silencing promotes cell proliferation in renal cancer crecursor cells

Cell-growth assays were performed. Both *Jade-1*-silenced cell lines grew faster than the non-silencing control cells (Figure 6A). In addition, BrdU incorporation assays revealed that silencing of *Jade-1* significantly increased cell proliferation 25-35% (Figure 6B). Thus, Jade-1 is involved in cell cycle progression and cell proliferation in renal cancer precursor cells.

Jade-1 silencing promotes anchorage-independent growth in renal cancer precursor cells

The PI3K/AKT pathway plays a key role in anchorage-independent growth, a key feature of transformed epithelia. Soft agar assays were performed on HK-2 cells, which normally do not grow in soft agar (28). Intriguingly, *Jade-1*-silenced HK-2 cells acquired the capacity for anchorage-independent survival and growth (Figure 6C). This capacity was inhibited by reintroduction of Jade-1 (Figure 6D) or LY294002 (Figure 6E); moreover, it was suppressed by dominant-negative AKT and enhanced by constitutively active myrAKT (Figure 6F). myrAKT alone was barely able to transform the non-silencing control cells (Figure 6F, upper right). Therefore, *Jade*-1-silenced renal cancer precursor cells exhibit phospho-AKT-dependent transformation.

Jade-1 message levels are low in clear-cell RCC, and low *Jade-1* is associated with worse patient features and activation of an AKT1 target-gene signature

We analyzed The Cancer Genome Atlas database for differential gene expression (p=0.001, false-discovery rate (FDR) <0.001) between clear-cell RCCs (n=65) and corresponding normal kidney tissue (n=65) from the same patient. *Jade-1* message, but not *AKT1* message, was significantly under-expressed in clear-cell RCC samples, with a ratio of 0.74. Furthermore, in all clear-cell RCCs in the database, low levels of *Jade-1* message (n=232) were significantly associated with advanced tumor stage, high pathological grade and more patient deaths, in comparison with clear-cell RCCs with high *Jade-1* expression (n=232) (Table 1). In contrast, *AKT1* message levels were not significantly associated with these clinical characteristics (data not shown). Most likely, *AKT1* transcript levels are not strongly correlated with active AKT1 protein levels. Importantly, the low *Jade-1*-expressing clear-cell RCC samples exhibited overexpression of genes positively regulated by AKT1 and underexpression of genes negatively regulated by AKT1 (Supplementary Table S1), consistent with the activation of an AKT1 target-gene signature (32, 33) under low *Jade-1* conditions.

Discussion

While most cases of clear-cell RCC involve inactivation of the pVHL tumor suppressor (1, 3), AKT is abnormally activated in about half of cases (8), sometimes due to PTEN mutation (9, 10) or more often from decreased PTEN expression (11-13). Other mechanisms for activation of AKT in RCC have been unknown, but cooperativity between the PTEN and pVHL pathways has been described (7). Jade-1 is a highly regulated, anti-proliferative and pro-apoptotic molecule enriched in kidney epithelial cells. Loss of Jade-1 stabilization by pVHL correlates with renal cancer risk (17). Here, we provide further evidence for the renal tumor suppressor role of Jade-1 as an inhibitor of phospho-AKT. Overexpression of Jade-1 decreased and silencing of *Jade-1* increased the level of endogenous phospho-AKT/AKT1 in renal cell lines. By increasing Jade-1 abundance, reintroduction of pVHL into renal cancer cells inhibited phospho-AKT. The N terminus of Jade-1 bound the catalytic domain and the C-terminal regulatory region of AKT. Levels of AKT downstream targets GSK3β S9 and p21 were upregulated in *Jade-1*-silenced renal cancer precursor cells, which showed increased proliferation and AKT-dependent anchorage-independent growth. myrAKT could not completely replace *Jade-1* silencing in anchorage-independent growth, implying that additional pathways are involved in the tumor suppressor activity of Jade-1, such as ubiquitination of β-catenin (19). Therefore the tumor suppressor function of Jade-1 is due in part to inhibition of AKT activity. We have also found that, in comparison with normal kidney, *Jade-1* message is significantly reduced in clear-cell renal cell carcinoma, which is associated with poor prognosis and activation of an AKT1 target-gene sequence, consistent with Jade-1 serving as a key regulator of the PI3K/AKT pathway.

Jade-1 abundance is low to undetectable in renal cancer cell lines but is high in differentiated renal proximal tubular cells (18). Our results show that when Jade-1 levels fall, hyperactivated AKT in renal cancer precursor cells could facilitate their survival and proliferation, and presumably make them less sensitive to apoptotic signals. The surviving cells might reprogram energy metabolism, for example, through GSK3β (34). These cells could outgrow other normal cells by manipulating cell cycle-related proteins, such as p21 and p27, to get a proliferation advantage. In addition, hyperactivated AKT in renal cancer precursor cells favors anchorage-independent growth, which is critical for epithelial-mesenchymal transition (EMT), a process through which epithelial cells acquire deregulated cell polarity, reduced intercellular adhesion, and increased invasion/metastasis. Thus, increased AKT activation could contribute to renal tumorigenesis in multiple ways.

AKT signaling is a ubiquitous eukaryotic pathway, and complex mechanisms exist for fine control of AKT. AKT-interacting proteins can modify AKT kinase activity or target specificity. For example, by binding the AKT PH domain, oncoprotein Tcl1 activates AKT and promotes its translocation to the nucleus (35). TRB3 binds the activation loop of the AKT kinase domain and inhibits AKT phosphorylation (36). CTMP binds specifically to the C-terminal regulatory region of AKT1 at the plasma membrane and negatively regulates AKT1 activation (37). The mechanism of Jade-1 inhibition of AKT may be unique because Jade-1 binds both the AKT kinase and regulatory domains.

AKT undergoes a substantial conformational change upon phosphorylation of T308 and S473 (38). Following this, ATP binding K179 in the catalytic cleft of AKT induces interactions between the phosphorylated sites and other residues such as H194 and R273 in the cleft, creating a “phosphatase shielding cage” (39, 40). ATP hydrolysis and substrate phosphorylation “uncage” AKT phosphorylated sites, leading to dephosphorylation and inactivation of AKT. An inherited AKT2 R274H mutation blocking “cage” formation leads to AKT2 kinase inhibition and results in severe diabetes mellitus in humans (41). The K179M mutation abolishes the ATP binding site, so AKT K179M adapts an “uncaged” conformation. Our data show that Jade-1 binds AKT K179M with much higher affinity than the other forms of AKT tested, suggesting that overexpressed Jade-1, through its strong retention of “uncaged” AKT, could facilitate phosphatase accessibility, leading to lower steady-state levels of endogenous phospho-AKT. This assumption is strengthened by our data: 1. Jade-1 binds both the AKT catalytic domain and C-terminal regulatory tail, implying Jade-1 may affect the AKT phosphorylation sites. 2. When cells are at confluence, colocalization of Jade-1 and AKT is highest near the cell membrane, where AKT phosphorylation occurs. A model of pVHL and Jade-1 control of phospho-AKT is presented (Figure 6G). Thus, as a tightly regulated short-lived protein, Jade-1 can provide fine control of AKT phosphorylation and thereby AKT activity.

Loss of PTEN plays an important role in RCC, but additional biomarkers are needed. The familial PTEN hamartoma and tumor syndrome (PHTS) results in a 30-fold increased risk of RCC (42). PTEN gene defects have been found in about 30% of RCCs (9, 10, 13, 43), which should increase phospho-AKT. A relationship between decreased PTEN expression and increased phospho-AKT has been identified in clear-cell, but not in papillary or chromophobe RCC (44). In an analysis of seven renal cancer cell lines, four *VHL* null and three *VHL* intact, all had constitutive phosphorylation of AKT (15), so there are likely to be more pathways to AKT activation in RCC than just PTEN or pVHL loss, such as decreased Jade-1, which we have observed in all RCC cell lines tested (18). Loss of PTEN may be a poor prognostic finding (11, 12), but PTEN, HIF-1alpha, CA9 or pVHL status have not proved to be useful predictive biomarkers for therapy with mTOR inhibitors (13, 43). Instead, phospho-S6 ribosomal protein and perhaps phospho-AKT were predictive markers for response to temsirolimus in RCC (13). Moreover, only patients with high levels of phospho-S6 or phospho-AKT responded to temsirolimus (13). Low levels of Jade-1 may prove to be a predictive biomarker for mTOR inhibitor therapy in RCC, as well as a prognostic biomarker.

pVHL is best understood as targeting the hypoxia-inducible factor α transcription factors for ubiquitination and proteasomal degradation (45); however, non-HIF pathways are important for phenotypes other than angiogenesis in VHL disease and renal cancer. This work indicates that pVHL fine tunes AKT kinase activity through stabilization of the short-lived protein Jade-1 in renal cancer precursor cells. In addition to Jade-1 regulation (16), pVHL can regulate NFκB activity and tumorigenesis by serving as an adaptor to promote the inhibitory phosphorylation of the NFκB agonist Card9 by kinase CK2 (46). pVHL has also been shown to regulate microtubules and primary cilium formation in kidney cells (47),

endocytosis of fibroblast growth factor receptor 1 (48) and assembly of extracellular matrix (49). The regulation of Jade-1 protein and hence AKT by pVHL thus sheds new light on the molecular events in clear-cell RCC subsequent to *VHL* loss. Furthermore, *Jade-1* expression appears to be dysregulated at the message level as well in clear-cell RCC through an unidentified mechanism. Candidate renal tumor suppressor Jade-1 is therefore a key regulator of multiple cell signaling pathways and normally prevents renal epithelial cell proliferation and transformation.

Supplementary Material

Refer to Web version on PubMed Central for supplementary material.

Acknowledgments

The authors thank Z. Xiao and K. Walsh for generously providing reagents; D. Faller, T. Hsu and Z. Luo for helpful discussions; R. Simon and colleagues for developing BRB-array tools (National Cancer Institute); and The Cancer Genome Atlas research network for producing and maintaining microarray databases.

Grants: This work was supported by NIH grants R01 CA079830 and R01 DK067569 to HTC, and NIH grants R37 DK51050 and R01 DK53357 and March of Dimes grant 1-FY12-527 to JZ.

References

1. Cohen HT, McGovern FJ. Renal-cell carcinoma. N Engl J Med. 2005; 353(23):2477–90. [PubMed: 16339096]
2. Siegel R, Naishadham D, Jemal A. Cancer statistics, 2013. CA Cancer J Clin. 2013; 63(1):11–30. [PubMed: 23335087]
3. Li L, Kaelin WG Jr. New insights into the biology of renal cell carcinoma. Hematol Oncol Clin North Am. 2011; 25(4):667–86. [PubMed: 21763962]
4. Latif F, Tory K, Gnarra J, Yao M, Duh FM, Orcutt ML, et al. Identification of the von Hippel-Lindau disease tumor suppressor gene. Science. 1993; 260(5112):1317–20. [PubMed: 8493574]
5. Gnarra JR, Tory K, Weng Y, Schmidt L, Wei MH, Li H, et al. Mutations of the VHL tumour suppressor gene in renal carcinoma. Nat Genet. 1994; 7(1):85–90. [PubMed: 7915601]
6. Manning BD, Cantley LC. AKT/PKB signaling: navigating downstream. Cell. 2007; 129(7):1261–74. [PubMed: 17604717]
7. Frew IJ, Thoma CR, Georgiev S, Minola A, Hitz M, Montani M, et al. pVHL and PTEN tumour suppressor proteins cooperatively suppress kidney cyst formation. EMBO J. 2008; 27(12):1747–57. [PubMed: 18497742]
8. Hager M, Haufe H, Kemmerling R, Hitzl W, Mikuz G, Moser PL, et al. Increased activated Akt expression in renal cell carcinomas and prognosis. J Cell Mol Med. 2009; 13(8B):2181–8. [PubMed: 18774962]
9. Steck PA, Pershouse MA, Jasser SA, Yung WK, Lin H, Ligon AH, et al. Identification of a candidate tumour suppressor gene, MMAC1, at chromosome 10q23.3 that is mutated in multiple advanced cancers. Nat Genet. 1997; 15(4):356–62. [PubMed: 9090379]
10. Ikediobi ON, Davies H, Bignell G, Edkins S, Stevens C, O'Meara S, et al. Mutation analysis of 24 known cancer genes in the NCI-60 cell line set. Mol Cancer Ther. 2006; 5(11):2606–12. [PubMed: 17088437]
11. Velickovic M, Delahunt B, McIver B, Grebe SK. Intragenic PTEN/MMAC1 loss of heterozygosity in conventional (clear-cell) renal cell carcinoma is associated with poor patient prognosis. Mod Pathol. 2002; 15(5):479–85. [PubMed: 12011252]
12. Shin Lee J, Seok Kim H, Bok Kim Y, Cheol Lee M, Soo Park C. Expression of PTEN in renal cell carcinoma and its relation to tumor behavior and growth. J Surg Oncol. 2003; 84(3):166–72. [PubMed: 14598361]

13. Cho D, Signoretti S, Dabora S, Regan M, Seeley A, Mariotti M, et al. Potential histologic and molecular predictors of response to temsirolimus in patients with advanced renal cell carcinoma. Clin Genitourin Cancer. 2007; 5(6):379–85. [PubMed: 17956710]
14. Morris ZS, McClatchey AI. Aberrant epithelial morphology and persistent epidermal growth factor receptor signaling in a mouse model of renal carcinoma. Proc Natl Acad Sci U S A. 2009; 106(24):9767–72. [PubMed: 19487675]
15. Sourbier C, Lindner V, Lang H, Agouni A, Schordan E, Danilin S, et al. The phosphoinositide 3-kinase/Akt pathway: a new target in human renal cell carcinoma therapy. Cancer Res. 2006; 66(10):5130–42. [PubMed: 16707436]
16. Zhou MI, Wang H, Ross JJ, Kuzmin I, Xu C, Cohen HT. The von Hippel-Lindau tumor suppressor stabilizes novel plant homeodomain protein Jade-1. J Biol Chem. 2002; 277(42):39887–98. [PubMed: 12169691]
17. Zhou MI, Wang H, Foy RL, Ross JJ, Cohen HT. Tumor suppressor von Hippel-Lindau (VHL) stabilization of Jade-1 protein occurs through plant homeodomains and is VHL mutation dependent. Cancer Res. 2004; 64(4):1278–86. [PubMed: 14973063]
18. Zhou MI, Foy RL, Chitalia VC, Zhao J, Panchenko MV, Wang H, et al. Jade-1, a candidate renal tumor suppressor that promotes apoptosis. Proc Natl Acad Sci U S A. 2005; 102(31):11035–40. [PubMed: 16046545]
19. Chitalia VC, Foy RL, Bachschmid MM, Zeng L, Panchenko MV, Zhou MI, et al. Jade-1 inhibits Wnt signalling by ubiquitylating beta-catenin and mediates Wnt pathway inhibition by pVHL. Nat Cell Biol. 2008; 10(10):1208–16. [PubMed: 18806787]
20. Panchenko MV, Zhou MI, Cohen HT. von Hippel-Lindau partner Jade-1 is a transcriptional co-activator associated with histone acetyltransferase activity. J Biol Chem. 2004; 279(53):56032–41. [PubMed: 15502158]
21. Foy RL, Chitalia VC, Panchenko MV, Zeng L, Lopez D, Lee JW, et al. Polycystin-1 regulates the stability and ubiquitination of transcription factor Jade-1. Hum Mol Genet. 2012; 21(26):5456–71. [PubMed: 23001567]
22. Lian X, Duan X, Wu X, Li C, Chen S, Wang S, et al. Expression and clinical significance of von Hippel-Lindau downstream genes: Jade-1 and beta-catenin related to renal cell carcinoma. Urology. 2012; 80(2):485, e7–13. [PubMed: 22516360]
23. Tzouanacou E, Tweedie S, Wilson V. Identification of Jade1, a gene encoding a PHD zinc finger protein, in a gene trap mutagenesis screen for genes involved in anteroposterior axis development. Mol Cell Biol. 2003; 23(23):8553–2. [PubMed: 14612400]
24. Voas MG, Rebay I. The novel plant homeodomain protein rhinoceros antagonizes Ras signaling in the Drosophila eye. Genetics. 2003; 165(4):1993–2006. [PubMed: 14704181]
25. Cui M, Chen J, Myers TR, Hwang BJ, Sternberg PW, Greenwald I, et al. SynMuv genes redundantly inhibit lin-3/EGF expression to prevent inappropriate vulval induction in C. elegans. Dev Cell. 2006; 10(5):667–72. [PubMed: 16678779]
26. Fujio Y, Guo K, Mano T, Mitsuuchi Y, Testa JR, Walsh K. Cell cycle withdrawal promotes myogenic induction of Akt, a positive modulator of myocyte survival. Mol Cell Biol. 1999; 19(7): 5073–82. [PubMed: 10373556]
27. Zhou GL, Tucker DF, Bae SS, Bhatheja K, Birnbaum MJ, Field J. Opposing roles for Akt1 and Akt2 in Rac/Pak signaling and cell migration. J Biol Chem. 2006; 281(47):36443–53. [PubMed: 17012749]
28. Ryan MJ, Johnson G, Kirk J, Fuerstenberg SM, Zager RA, Torok-Storb B. HK-2: an immortalized proximal tubule epithelial cell line from normal adult human kidney. Kidney Int. 1994; 45(1):48–57. [PubMed: 8127021]
29. Shiojima I, Walsh K. Regulation of cardiac growth and coronary angiogenesis by the Akt/PKB signaling pathway. Genes Dev. 2006; 20(24):3347–65. [PubMed: 17182864]
30. Mayo LD, Donner DB. A phosphatidylinositol 3-kinase/Akt pathway promotes translocation of Mdm2 from the cytoplasm to the nucleus. Proc Natl Acad Sci U S A. 2001; 98(20):11598–603. [PubMed: 11504915]
31. Zhou BP, Liao Y, Xia W, Zou Y, Spohn B, Hung MC. HER-2/neu induces p53 ubiquitination via Akt-mediated MDM2 phosphorylation. Nat Cell Biol. 2001; 3(11):973–82. [PubMed: 11715018]

32. Kuhn I, Bartholdi MF, Salamon H, Feldman RI, Roth RA, Johnson PH. Identification of AKT-regulated genes in inducible MERAkt cells. Physiol Genomics. 2001; 7(2):105–14. [PubMed: 11773597]
33. Tiwari G, Sakaue H, Pollack JR, Roth RA. Gene expression profiling in prostate cancer cells with Akt activation reveals Fra-1 as an Akt-inducible gene. Mol Cancer Res. 2003; 1(6):475–84. [PubMed: 12692267]
34. Cohen P, Frame S. The renaissance of GSK3. Nat Rev Mol Cell Biol. 2001; 2(10):769–76. [PubMed: 11584304]
35. Pekarsky Y, Koval A, Hallas C, Bichi R, Tresini M, Malstrom S, et al. Tcl1 enhances Akt kinase activity and mediates its nuclear translocation. Proc Natl Acad Sci U S A. 2000; 97(7):3028–33. [PubMed: 10716693]
36. Du K, Herzig S, Kulkarni RN, Montminy M. TRB3: a tribbles homolog that inhibits Akt/PKB activation by insulin in liver. Science. 2003; 300(5625):1574–7. [PubMed: 12791994]
37. Maira SM, Galetic I, Brazil DP, Kaech S, Ingley E, Thelen M, et al. Carboxyl-terminal modulator protein (CTMP), a negative regulator of PKB/Akt and v-Akt at the plasma membrane. Science. 2001; 294(5541):374–80. [PubMed: 11598301]
38. Kumar CC, Madison V. AKT crystal structure and AKT-specific inhibitors. Oncogene. 2005; 24(50):7493–501. [PubMed: 16288296]
39. Chan TO, Zhang J, Rodeck U, Pascal JM, Armen RS, Spring M, et al. Resistance of Akt kinases to dephosphorylation through ATP-dependent conformational plasticity. Proc Natl Acad Sci U S A. 2011; 108(46):E1120–7. [PubMed: 22031698]
40. Lin K, Lin J, Wu WI, Ballard J, Lee BB, Gloor SL, et al. An ATP-site on-off switch that restricts phosphatase accessibility of Akt. Sci Signal. 2012; 5(223):ra37. [PubMed: 22569334]
41. George S, Rochford JJ, Wolfrum C, Gray SL, Schinner S, Wilson JC, et al. A family with severe insulin resistance and diabetes due to a mutation in AKT2. Science. 2004; 304(5675):1325–8. [PubMed: 15166380]
42. Tan MH, Mester JL, Ngeow J, Rybicki LA, Orloff MS, Eng C. Lifetime cancer risks in individuals with germline PTEN mutations. Clin Cancer Res. 2012; 18(2):400–7. [PubMed: 22252256]
43. Figlin RA, de Souza P, McDermott D, Dutcher JP, Berkenblit A, Thiele A, et al. Analysis of PTEN and HIF-1alpha and correlation with efficacy in patients with advanced renal cell carcinoma treated with temsirolimus versus interferon-alpha. Cancer. 2009; 115(16):3651–60. [PubMed: 19526589]
44. Hara S, Oya M, Mizuno R, Horiguchi A, Marumo K, Murai M. Akt activation in renal cell carcinoma: contribution of a decreased PTEN expression and the induction of apoptosis by an Akt inhibitor. Ann Oncol. 2005; 16(6):928–33. [PubMed: 15851405]
45. Maxwell PH, Wiesener MS, Chang GW, Clifford SC, Vaux EC, Cockman ME, et al. The tumour suppressor protein VHL targets hypoxia-inducible factors for oxygen-dependent proteolysis. Nature. 1999; 399(6733):271–5. [PubMed: 10353251]
46. Yang H, Minamishima YA, Yan Q, Schlisio S, Ebert BL, Zhang X, et al. pVHL acts as an adaptor to promote the inhibitory phosphorylation of the NF-kappaB agonist Card9 by CK2. Mol Cell. 2007; 28(1):15–27. [PubMed: 17936701]
47. Hergovich A, Lisztwan J, Barry R, Ballschmieter P, Krek W. Regulation of microtubule stability by the von Hippel-Lindau tumour suppressor protein pVHL. Nat Cell Biol. 2003; 5(1):64–70. [PubMed: 12510195]
48. Hsu T, Adereth Y, Kose N, Dammai V. Endocytic function of von Hippel-Lindau tumor suppressor protein regulates surface localization of fibroblast growth factor receptor 1 and cell motility. J Biol Chem. 2006; 281(17):12069–80. [PubMed: 16505488]
49. Ohh M, Yauch RL, Lonergan KM, Whaley JM, Stemmer-Rachamimov AO, Louis DN, et al. The von Hippel-Lindau tumor suppressor protein is required for proper assembly of an extracellular fibronectin matrix. Mol Cell. 1998; 1(7):959–68. [PubMed: 9651579]
50. Kirber MT, Chen K, Keaney JF Jr. YFP photoconversion revisited: confirmation of the CFP-like species. Nat Methods. 2007; 4(10):767–8. [PubMed: 17901864]

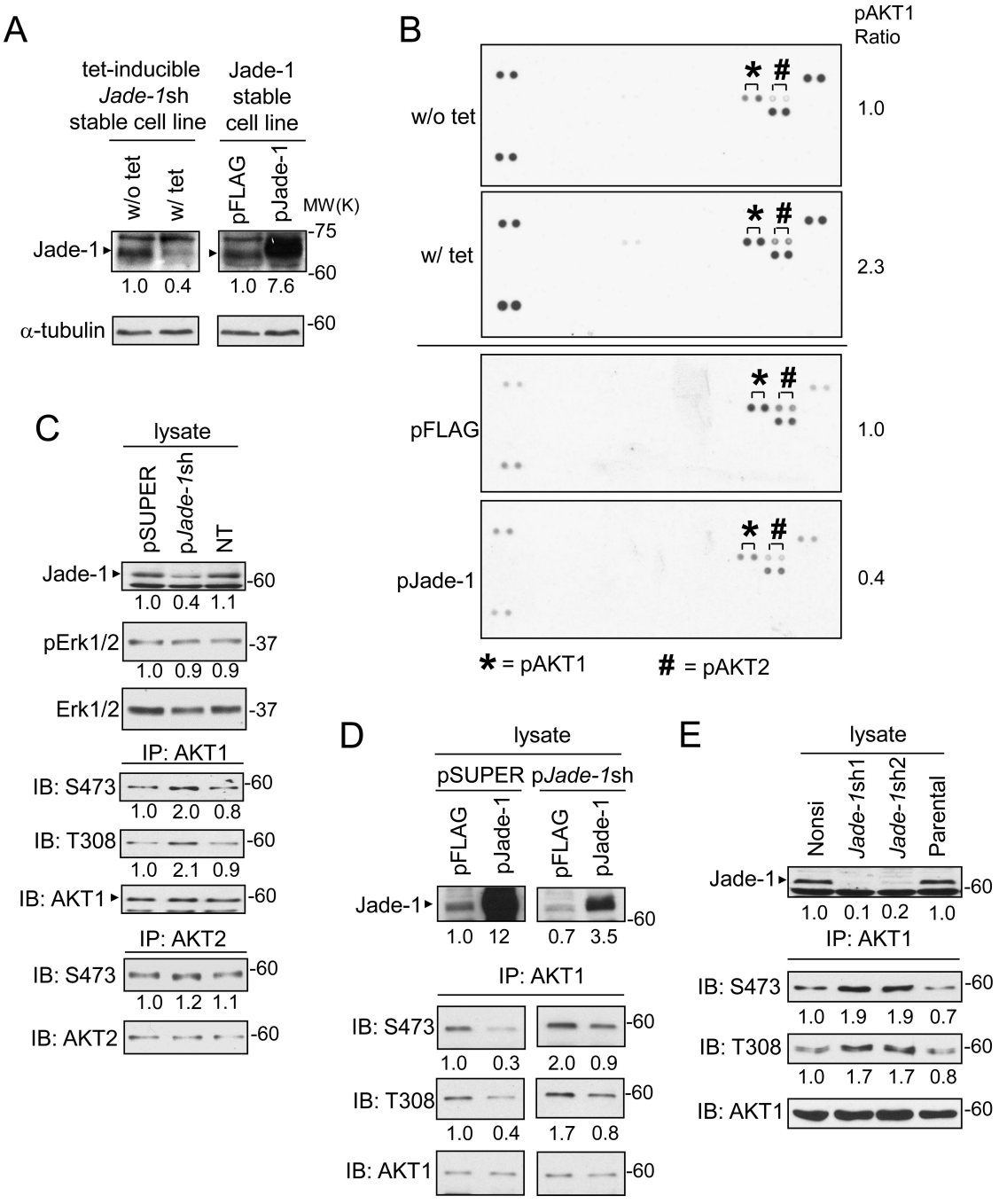

Figure 1.

Jade-1 regulates the level of endogenous phospho-AKT1. **A.** Jade-1 protein abundance was confirmed by immunoblot in tetracycline-inducible *Jade-1* knockdown HEK293 cells without (w/o) and with (w/) tetracycline (tet) and Jade-1 overexpression stable HEK293 cell lines. **B.** Cellular extracts prepared from inducible *Jade-1* knockdown HEK293 cells (w/o tet and w/ tet) and from empty vector (pFLAG) or Jade-1 overexpression (pJade-1) HEK293 stable cell lines were used in a MAPK array kit. The paired dots representing endogenous phospho-AKT1 (S473) are marked with *, and phospho-AKT2 (S474) with #. **C.** HEK293T cells were transiently transfected with empty vector (pSUPER), p*Jade-1*sh vector or non-targeting vector (NT). Cell extracts were analyzed for Jade-1, pErk1/2, and Erk1/2.

Endogenous AKT1 and AKT2 were immunoprecipitated from cell lysates and then detected with phospho-AKT antibody. **D.** HEK293T cells were transiently transfected with either pSUPER or p*Jade-1*sh first, followed by transfection with either pFLAG control vector or pJade-1 expression vector. **E.** Cell lysates were prepared from renal proximal tubule HK-2 stable cell lines non-silencing (nonsi) control, *Jade-1*sh1, *Jade-1*sh2 or parental control, then assessed for endogenous phospho-AKT1.

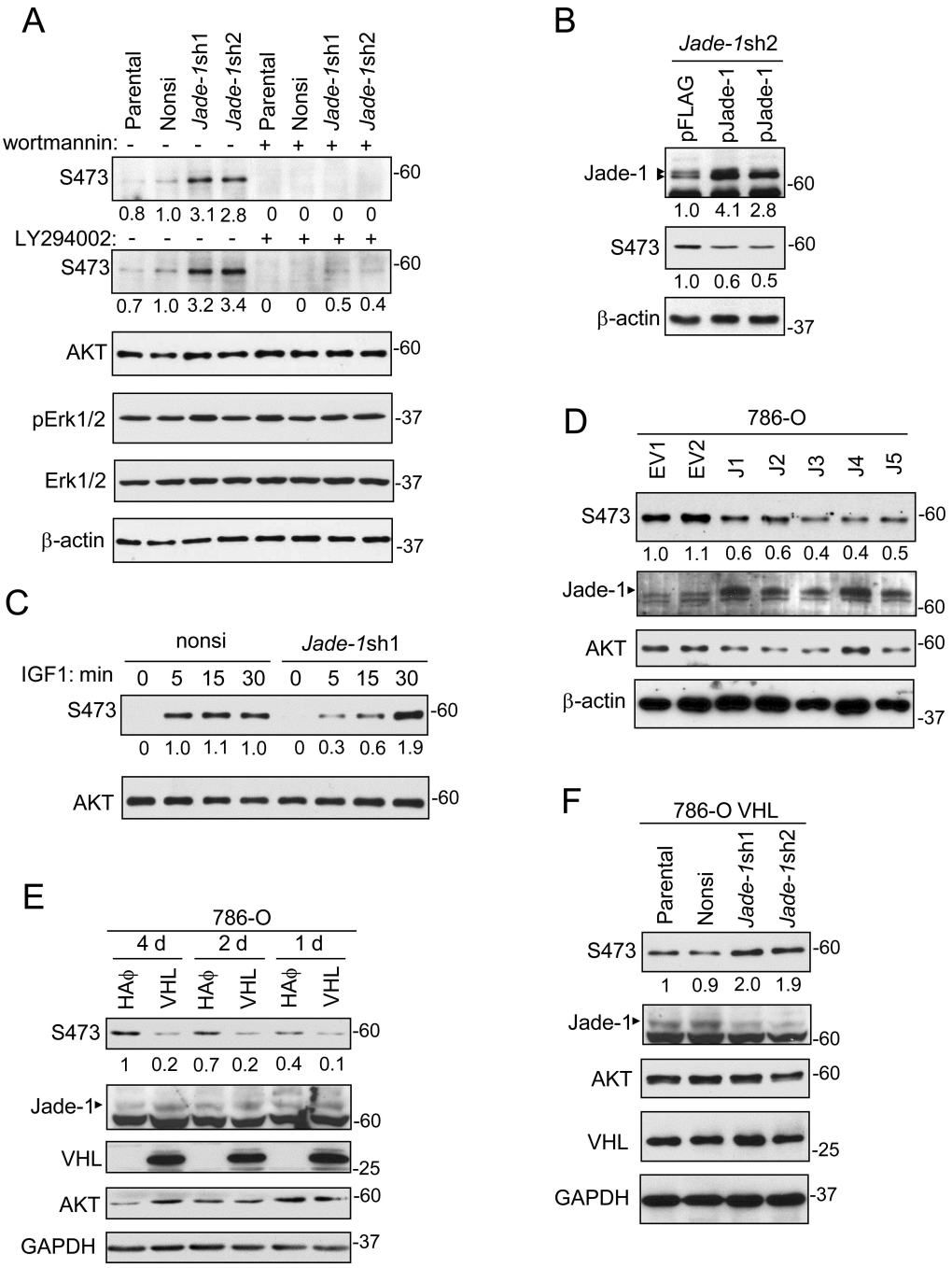

Figure 2.

Jade-1 regulates levels of endogenous phospho-AKT. **A.** *Jade-1* silencing increased the level of endogenous phospho-AKT in HK-2 cells. This effect was blocked by wortmannin or LY294002. By immunoblotting, pErk1/2 and Erk1/2 were also not affected by *Jade-1* silencing in the absence or presence of LY294002. **B.** The effect of *Jade-1* silencing on phospho-AKT was suppressed by a silencing-resistant Jade-1 vector (pJade-1). **C.** Nonsi and *Jade-1*-sh1 cells were starved for 16 hours then stimulated with 20 ng/mL IGF-1 for times shown. **D.** Stable overexpression of Jade-1 in 786-O renal cancer cell clonal lines inhibited endogenous phospho-AKT. **E.** Stable expression of pVHL in renal cancer cells increases

endogenous Jade-1 and decreases endogenous phospho-AKT. The 786-O stable cell line pools expressing either HA empty vector or HA-pVHL were examined for endogenous phospho-AKT four days, two days, and one day after confluence. **F.** The effect of pVHL on phospho-AKT is Jade-1 dependent. The 786-O VHL cells were transduced with nonsi, p*Jade-1*sh1 or p*Jade-1*sh2 containing virus and then examined for endogenous phospho-AKT.

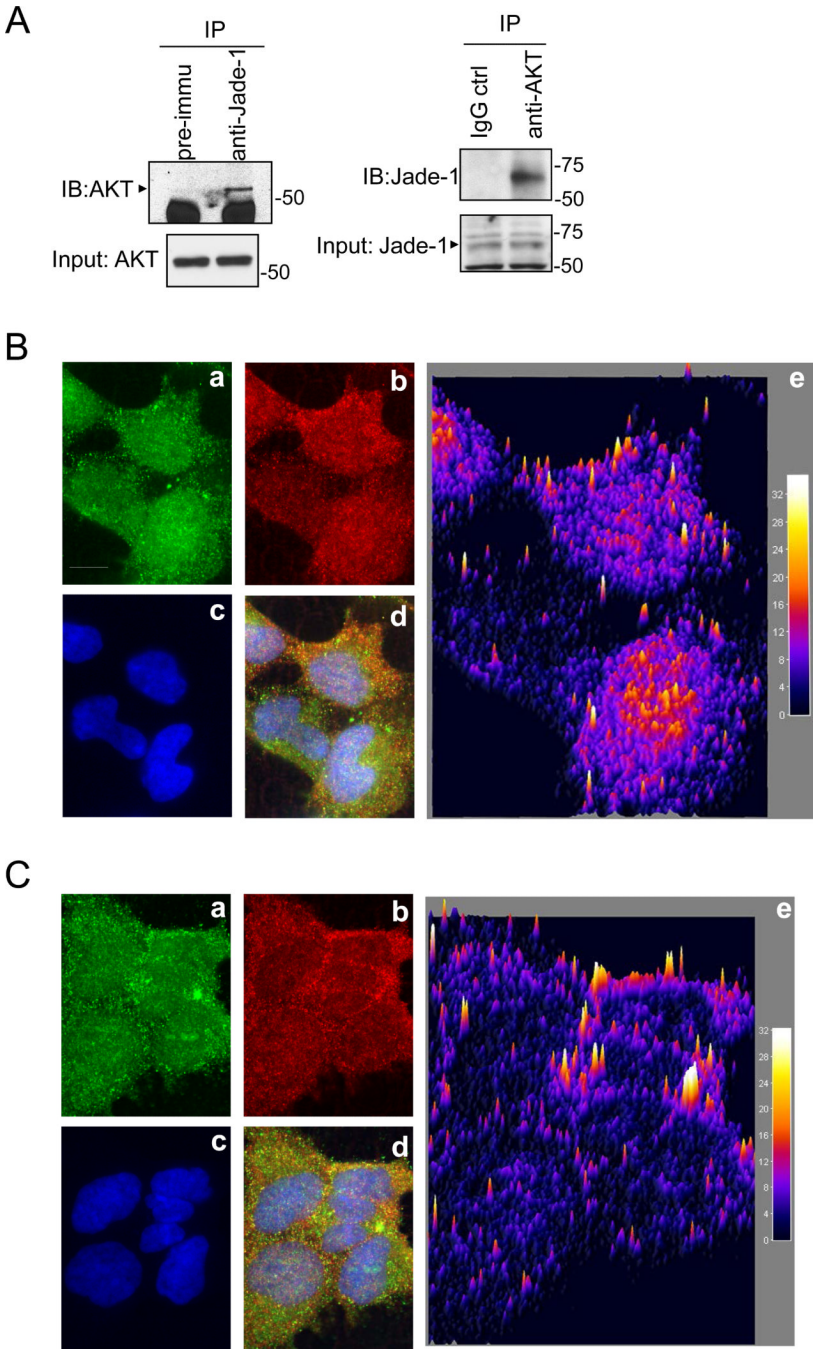

Figure 3.

Jade-1 binds AKT. **A.** Coimmunoprecipitation of endogenous AKT with endogenous Jade-1 in HK-2 cells. Immunoprecipitation was performed with either pre-immune rabbit serum or anti-Jade-1 rabbit polyclonal serum. Coimmunoprecipitated AKT was detected by immunoblotting with anti-AKT antibody. Likewise, cell lysates were also immunoprecipitated with AKT antibody first and then immunoblotted with Jade-1 antibody. **B.** Jade-1 and AKT partially colocalize intracellularly when cells are subconfluent. A representative confocal image is shown. All image processing was done with NIH ImageJ. a. Jade-1 fluorescence; b. AKT fluorescence; c. DAPI fluorescence; d. merged image of a, b and c; e. surface plot display of the normalized covariance image between a and b

(Interactive 3D surface plot plug-in for ImageJ, K. Barthel, Internationale Medieninformatick, Berlin, Germany) (50). Scale bar indicates 5 μm. Color bars show colocalized fluorescence intensity. **C.** Jade-1 and AKT colocalize predominantly at the plasma membrane at cell confluence. A representative confocal image is shown. a. Jade-1 fluorescence; b. AKT fluorescence; c. DAPI fluorescence; d. merged image of a, b and c; e. surface plot display of the normalized covariance image between a and b.

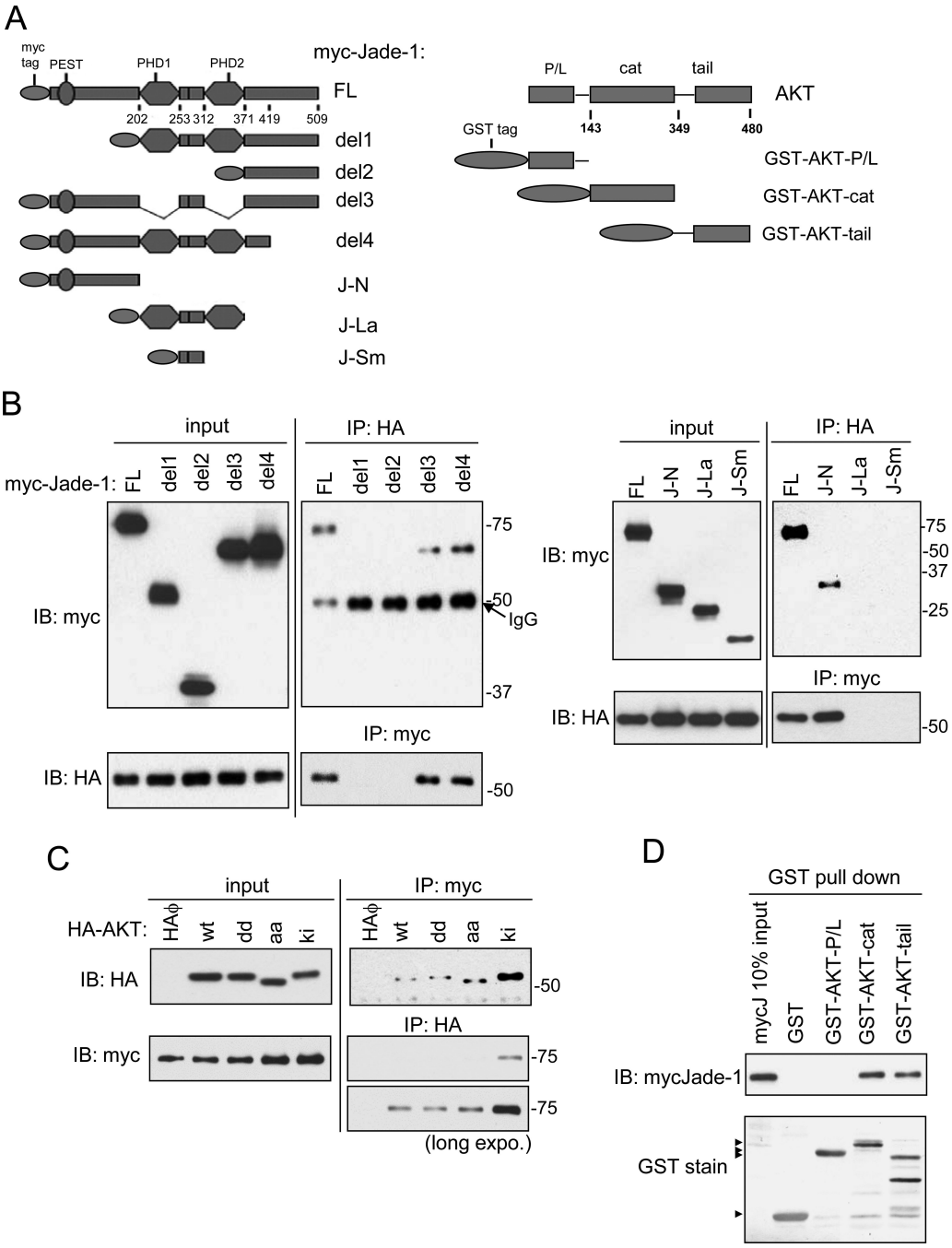

Figure 4.

The N-terminus of Jade-1 binds both the catalytic domain and the C-terminal regulatory region of AKT. **A.** Schematics of myc-tagged Jade-1 truncation constructs and GST-tagged AKT domain constructs. **B.** AKT binds the N terminus of Jade-1. HA-AKT was transiently cotransfected in HEK293T cells with myc-Jade-1 truncations (left panels: full length, del1, del2, del3, del4; and right panels: full length, J-N, J-La, J-Sm). Cell lysates were immunoprecipitated with anti-myc antibody and then immunoblotted with anti-HA antibody, and *vice versa*. Whole cell lysates (10% of input) showed comparable expression of HA-AKT or myc-Jade-1 truncations across samples. **C.** Jade-1 shows increased binding to a kinase inactive AKT mutant. Myc-Jade-1 was transiently cotransfected with different

forms of HA-AKT, wild type (wt); T308D/S473D (dd); T308A/S473A (aa); or K179M (ki). **D.** Jade-1 binds to the AKT kinase domain and the regulatory C terminus. Cell lysates with overexpressed myc-Jade-1 were incubated with bacterially expressed, purified GST fusion protein GST-AKT-P/L, GST-AKT-cat, GST-AKT-tail, or GST alone.

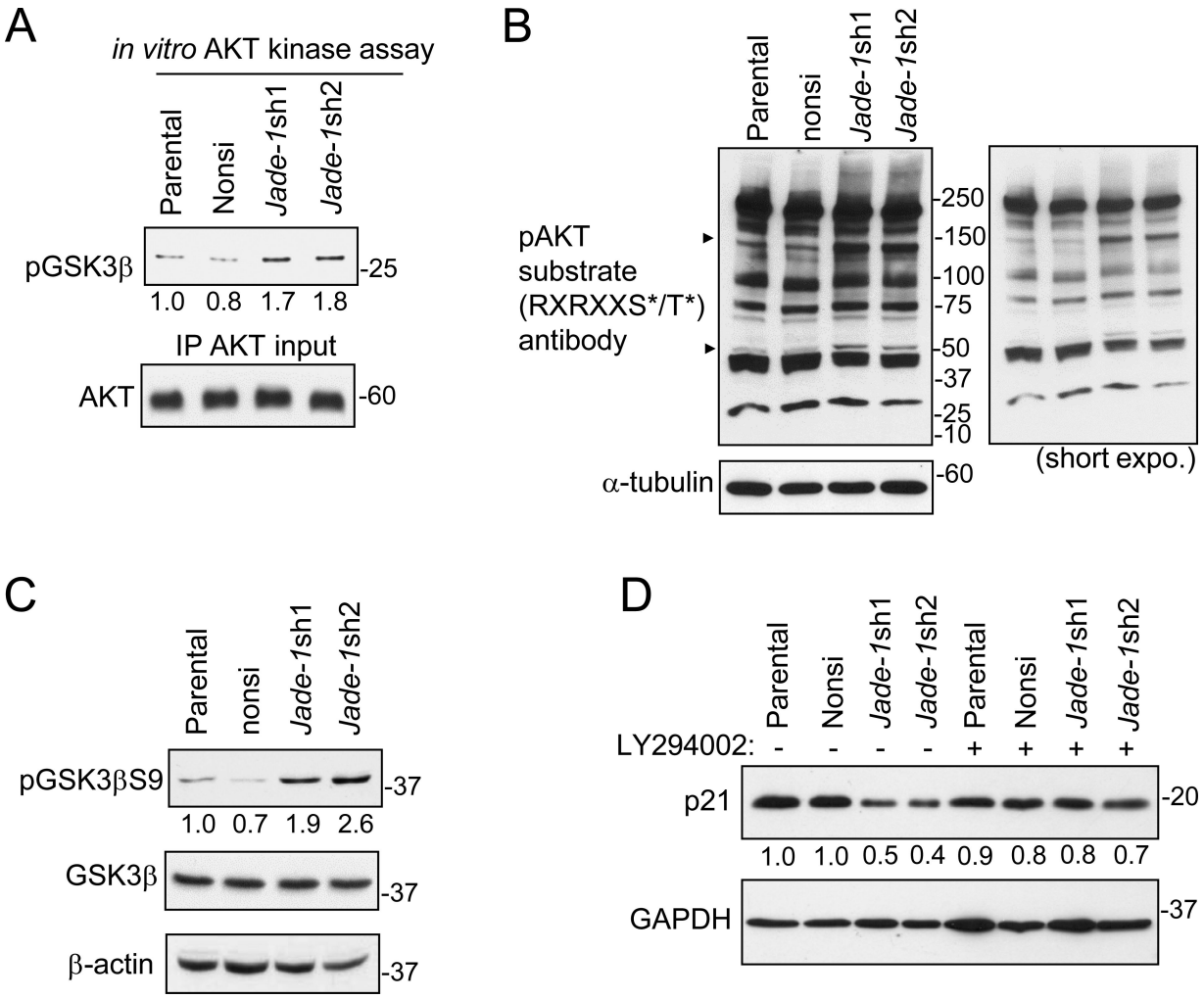

Figure 5.

AKT activity and levels of endogenous phospho-substrates of AKT are increased in *Jade-1*-silenced HK-2 cells. **A.** Endogenous AKT was immunoprecipitated from cellular extracts of HK-2 stable cell lines and then incubated with purified GSK3β substrate. The amount of phosphorylated GSK3β S9 was assessed by immunoblotting. **B.** Cell lysates from HK-2 cell lines were probed with a phospho-AKT substrate antibody. **C.** Levels of endogenous phospho-GSK3β S9, a known substrate of phospho-AKT, were assessed by immunoblot. **D.** Levels of endogenous p21 in the HK-2 cell lines were assessed without or with LY294002.

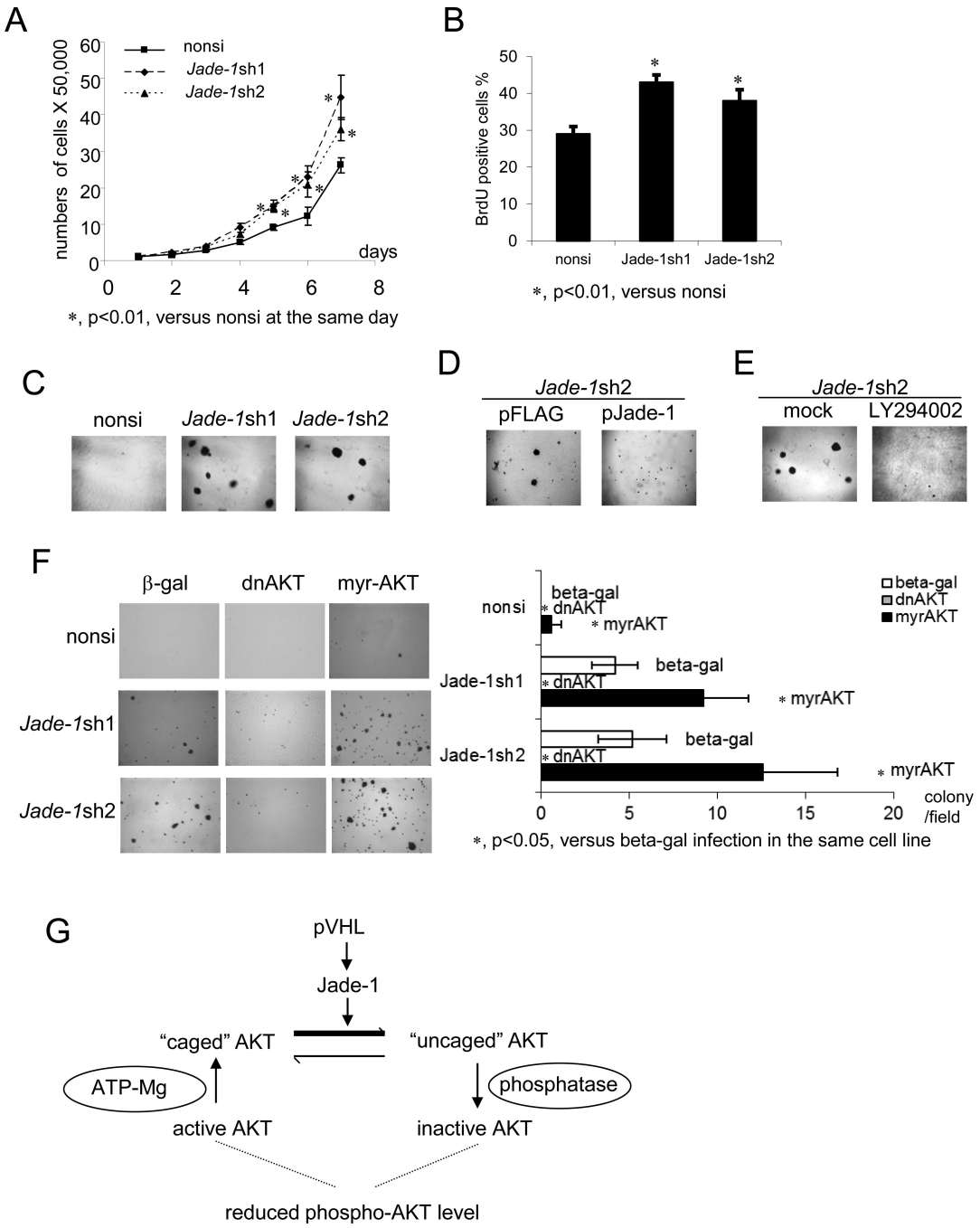

Figure 6.

Silencing of *Jade-1* increases cell proliferation and promotes AKT-dependent anchorage-independent growth. **A.** Cell numbers were counted with a hemocytometer for seven consecutive days. Error bars indicate SD. **B.** Growing cells were labeled with BrdU solution (10 μM, 1.5 hours). Incorporated BrdU was detected with anti-BrdU-POD solution (Roche) and visualized with 3, 3'-diaminobenzidine (DAB) substrate (Vector Laboratories). Error bars indicate SD. **C.** *Jade-1*-silenced HK-2 cell lines formed colonies in soft agarose. HK-2 cell lines were grown in an agarose suspension. Formation of colonies was monitored microscopically. **D.** Reintroduction of Jade-1 into *Jade-1*sh2 cells inhibited anchorage-

independent growth. **E.** LY294002 inhibited anchorage-independent growth of *Jade-1*sh2 cells. **F.** Anchorage-independent growth of *Jade-1* silenced HK-2 cells is AKT-dependent. HK-2 stable cell lines were infected with adenovirus expressing either β-gal control, dominant-negative AKT (dnAKT), or constitutively active AKT (myr-AKT) before they were suspended in soft agarose. Error bars indicate SD. **G.** A model of AKT inhibition by Jade-1/pVHL. Starting on the lower left, serine/threonine kinase AKT is activated by phosphorylation on T308 and S473. Binding of ATP in the catalytic cleft promotes formation of a stabilized form of AKT in which the phosphorylated residues are protected in a "phosphatase shielding cage". With AKT phosphorylation of a substrate protein and ATP hydrolysis, AKT adopts an "uncaged" conformation that is more susceptible to dephosphorylation and inactivation. Short-lived protein Jade-1 is stabilized by pVHL. During AKT activation, increased Jade-1 preferentially binds "uncaged" AKT, shifting the balance toward this form of phospho-AKT that is more susceptible to inactivation by phosphatases. Conversely, in renal cancer, loss of Jade-1/pVHL would shift the balance toward the "caged" form of AKT, resulting in higher phospho-AKT levels and increased AKT kinase activity.

Table 1

Patient clinical characteristics based on *Jade-1* gene expression.

Patient characteristics	Low *Jade-1* Expression (n=232)	High *Jade-1* Expression (n=232)	p-value (Chi-square)
Age (Years)			
Median	61	61	
Mean	60.85	60.44	ns[1]
Gender			
Female	86	75	
Male	146	157	ns[1]
Tumor Histological Grades			
GX	1	4	
G1	2	5	
G2	76	122	
G3	101	80	
G4	51	21	p<0.0001
Tumor Stages			
I	93	130	
II	23	24	
III	74	44	
IV	42	34	p=0.001
Survival			
Alive	141	172	
Dead	91	60	p=0.005

ns[1]= not significant